Progress In Electromagnetics Research C, Vol. 37, 119–130, 2013

DUAL-MODE DUAL-BAND BANDPASS FILTER BASED ON SQUARE LOOP RESONATOR

Kun Deng*, Shuai Yang, Shoujia Sun, Bian Wu, and Xiaowei Shi

National Laboratory of Science and Technology on Antennas and Microwaves, Xidian University, Xi'an, Shaanxi 710071, P. R. China

Abstract—In this paper, a dual-mode dual-band microstrip bandpass filter utilizing asymmetric square loop resonators is proposed. A pair of bent open-circuited stubs is installed to the loop as perturbation stubs. By stretching the perturbation stubs more than half-wavelength of the loop, the degenerated modes in a loop are split for dual-band operation. Two asymmetric resonators are cascaded to form two bands. Even- and odd-mode analysis method is used to deduce the resonant frequencies of two bands. Based on the transmission line theory, resonant frequencies of the two resonances are derived. According to the resonant conditions, a kind of dual-mode dual-band bandpass filter can be easily designed. Finally, a dual-band filter with two bands centering at 1.9 GHz and 2.6 GHz is designed in a comprehensive way. Measured results of experimental circuit show good agreement with simulated responses.

1. INTRODUCTION

In recent years, dual-band bandpass filter design has been a hot research topic. The initial type of dual-band filter is usually designed by connecting two filter circuits with two different passbands [1]. Many papers show that several approaches have been developed for achieving dual-band operation in bandpass filters [2–12]. In [2], a dual-band bandpass filter using resonators based on slotted ground structures is demonstrated. Dual-band filters using split-ring resonators can be seen in [3, 4]. Stepped impedance resonators (SIRs) [5] and coupled lines [6, 7] can also be utilized to design dual-band filters. Dual-mode

Received 6 January 2013, Accepted 30 January 2013, Scheduled 1 February 2013
* Corresponding author: Kun Deng (dengkun139@gmail.com).

dual-band filters based on Loop/ring resonators were described in [8–10] and similar triangular resonators were depicted in [11]. Of them, the dual-mode dual-band filters using loop/ring resonators have been paid more attention to because of their advantages such as small size, low loss.

The motivation of this paper is to give a unified description on the operating principle and design procedure of a novel dual-mode dual-band loop resonator bandpass filter. The initial concept was proposed in [12] through equivalent-circuit model and the solutions need complex calculations. In this paper, the behavior of the dual-mode dual-band bandpass filter will be characterized in a comprehensive way by transmission line theory. The design method proposed in this paper is found to be simple and flexible.

2. FILTER DESIGN

The resonator for the proposed filter is shown in Fig. 1(a). It is a symmetric structure, θ_i ($i = 1, 2, 3, 4$) represents the electric length of each segment, L_i ($i = 1, 2, 3, 4$) is the physical length of θ_i. Z_1 and Z_2 are the impedances of the perturbation stub and the loop resonator, respectively. Even and odd analysis method is used to derive the resonant frequencies. With the even- and odd-mode excitations at two ports, the dash line can be considered as a perfect magnetic wall and electric wall. Figs. 1(b) and (c) show the even- and odd-mode equivalent circuits. Ignoring the impact of the discontinuity and open-edge capacitance, when even mode motivates, the input impedance is

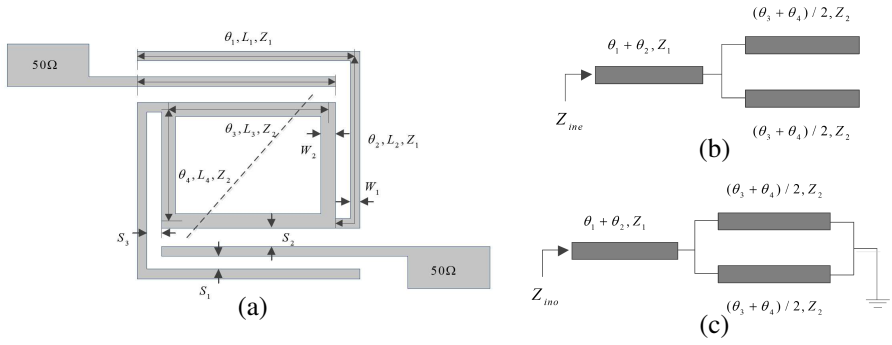

Figure 1. (a) Initial resonator for dual-mode dual-band bandpass filter. (b) Even mode of the equivalent circuit model. (c) Odd mode of the equivalent circuit model.

given below:

$$Z_{ine} = jZ_1 \frac{2Z_1 \tan(\theta_1 + \theta_2) - Z_2 \cot[(\theta_3 + \theta_4)/2]}{2Z_1 + Z_2 \cot[(\theta_3 + \theta_4)/2] \cdot \tan(\theta_1 + \theta_2)} \tag{1}$$

When odd mode motivates, the input impedance can be expressed as following:

$$Z_{ino} = jZ_1 \frac{2Z_1 \tan(\theta_1 + \theta_2) + Z_2 \tan[(\theta_3 + \theta_4)/2]}{2Z_1 - Z_2 \tan(\theta_1 + \theta_2) \cdot \tan[(\theta_3 + \theta_4)/2]} \tag{2}$$

The resonant frequencies can be obtained when the input admittances of even and odd modes, i.e., Y_{ine} and Y_{ino} are zero. The resonant conditions for the proposed filter can be expressed as below

$$2R_Z + \tan(\theta_1 + \theta_2) \cdot \cot[(\theta_3 + \theta_4)/2] = 0 \quad \text{for even mode} \tag{3}$$

$$2R_Z - \tan(\theta_1 + \theta_2) \cdot \tan[(\theta_3 + \theta_4)/2] = 0 \quad \text{for odd mode} \tag{4}$$

where $R_Z = Z_1/Z_2$.

From the resonant conditions, we know that the resonances depend on R_Z, $\theta_1 + \theta_2$ and $\theta_3 + \theta_4$. It is well known that there are two degenerate orthogonal modes, TM_{10} and TM_{o1}, coexisting in a loop resonator. The two degenerate modes will be split when various forms of perturbations are added to the loop resonator, still with their higher order degenerate modes. When the perturbation stubs of the resonator in Fig. 1(a) are stretched, the first and second-order degenerate modes are split, which can be used for dual-band bandpass filter design.

Figure 2 plots the normalized resonant frequencies of the first even and odd modes, f_{e1}/f_0 and f_{o1}/f_0 versus the length ratio of $k = (\theta_1 + \theta_2)/(\theta_3 + \theta_4)$ in the range of $[1, 1.5]$ under the impedance

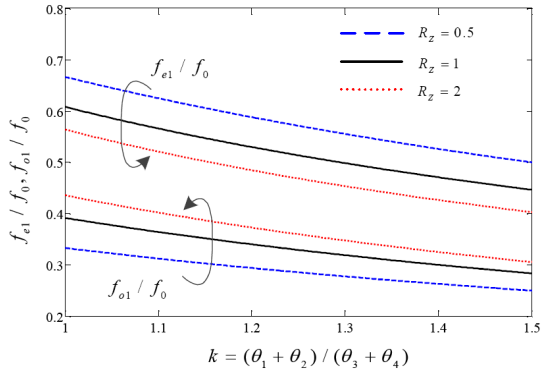

Figure 2. Normalized resonant frequencies of the first even and odd modes versus normalized stub length with different impedance ratios.

ratio of $R_Z = 0.5$, 1 and 2, where f_0 is the fundamental resonance of the loop resonator. It can be seen that when R_Z increases, the frequency separation of $f_{e1} - f_{o1}$, i.e., $f_2 - f_1$ decreases, and vice versa. This trend allows us to design a filter with different frequencies. Fig. 3 depicts the frequency ratio of f_{e1}/f_{o1}, i.e., f_2/f_1 versus the length ratio of $k = (\theta_1 + \theta_2)/(\theta_3 + \theta_4)$ under different impedance ratio of R_Z from 0.2 to 4. From the figure, it can be found that the frequency ratio of f_{e1}/f_{o1} has a large value when R_Z is small, and it decreases fast when R_Z increases from 0.2 to 1, the decreasing speed begin to slow down when R_Z keeps increasing from 1 to 4. Meanwhile, f_{e1}/f_{o1} keeps almost unchanged while R_Z is fixed no matter what the length ratio of $k = (\theta_1 + \theta_2)/(\theta_3 + \theta_4)$ is in the range of $[1, 1.5]$. Different frequency ratio of f_{e1}/f_{o1} can be figured out from Fig. 3 and thus be used to design filter. Our design goal is a dual-band filter resonating at 1.9 GHz and 2.6 GHz. Firstly, select the electric length ratio of $k = (\theta_1 + \theta_2)/(\theta_3 + \theta_4)$, the initial value of k should be set in the range of $[1.2, 1.4]$. The range is obtained based on lots of simulations, so it is an experiential value. We choose the value of k as 1.25. Then the frequency ratio can be calculated and it is $2.6/1.9 \approx 1.37$. The impedance ratio is determined from Fig. 3 under $k = 1.25$ and $f_{e1}/f_{o1} = 1.37$, and $R_Z \approx 1.3$. By this time, the wanted line widths of the perturbation stub and the loop resonator can be set, and the parameters are : $W_1 = 0.4$ mm, $W_2 = 0.8$ mm. The impedances of the two lines can be calculated on a substrate with the dielectric constant $\varepsilon_r = 2.65$ and thickness $h = 1$ mm, and that $Z_1 = 127.7$, $Z_2 = 97.6$, $R_Z \approx 1.3$. Secondly, plot the normalized resonant frequencies versus normalized stub length according to (3) and (4), which is shown in Fig. 4. From the figure, it can be seen that both of the first even mode f_{e1} ($f_{e1} = 2f_0$, when $\theta_1 + \theta_2 = 0$) and the first odd mode f_{o1} decrease fast as k increases, and that both of the two frequencies decrease to be a lower position than the fundamental resonance f_0 of the loop resonator when the normalized length ratio of k is larger than 0.5. Two normalized frequencies can be read from the figure at the certain position of $k = 1.25$, which shows that $f_{o1}/f_0 = 0.3503$ and $f_{e1}/f_0 = 0.4881$. By this time, the fundamental resonant frequency of the loop resonator can be determined through the following expression,

$$f_0 = (f_2 - f_1)/(f_{e1}/f_0 - f_{o1}/f_0) \tag{5}$$

Substrate $f_2 = 2.6$ GHz, $f_1 = 1.9$ GHz, $f_{e1}/f_0 = 0.4881$ and $f_{o1}/f_0 = 0.3503$ into (5), $f_0 = 5.08$ GHz can be figured out. The guided wavelength λ_0 is 41.8 mm. It means the initial physical dimensions of the proposed filter have been known once the guided wavelength of the loop resonator is obtained. We define the initial dimensions of the filter as follows: $L_3 = 12$ mm, $L_4 = 9$ mm, $L_2 = 11.5$ mm,

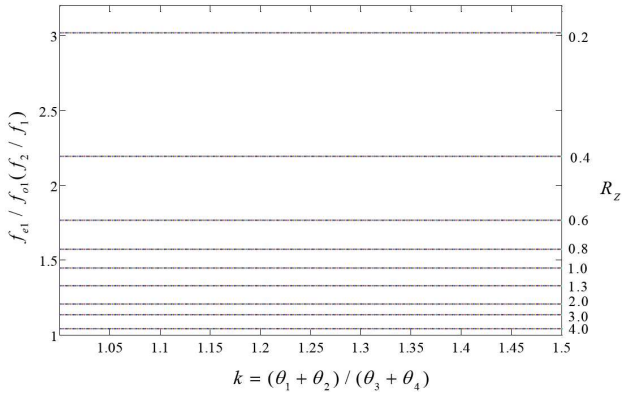

Figure 3. Frequency ratio of f_{e1}/f_{o1} versus normalized stub length with different impedance ratios.

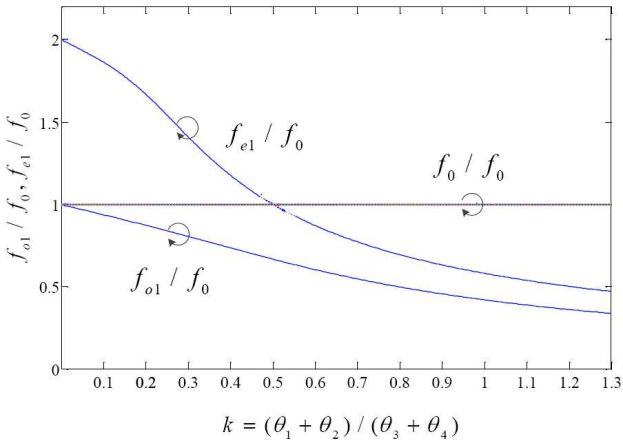

Figure 4. Normalized even and odd mode resonant frequencies versus normalized stub length.

$L_1 = 14.5\,\text{mm}$. The defined parameters satisfy $L_3 + L_4 \approx \lambda_0/2$ and $(L_1 + L_2)/(L_3 + L_4) \approx k$. Fig. 5 plots the simulated results of the frequency response of the resonator with initial parameters, we can find that the first resonance resonates at 1.88 GHz and the second resonance resonates at 2.53 GHz.

Two resonators are cascaded for dual-band operation, which is shown in Fig. 6. The cascaded structure may destroy the symmetry of the perturbation stubs if the end of the perturbation is beyond the

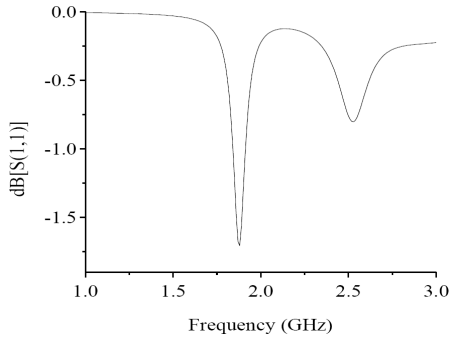

Figure 5. Frequency response of the initial resonator. (Dimensions are: $L_1 = 14.5\,\text{mm}$, $L_2 = 11.5\,\text{mm}$, $L_3 = 12\,\text{mm}$, $L_4 = 9\,\text{mm}$, $W_1 = 0.4\,\text{mm}$, $W_2 = 0.8\,\text{mm}$, $S_1 = 0.2\,\text{mm}$, $S_2 = 0.7\,\text{mm}$, $S_3 = 0.4\,\text{mm}$).

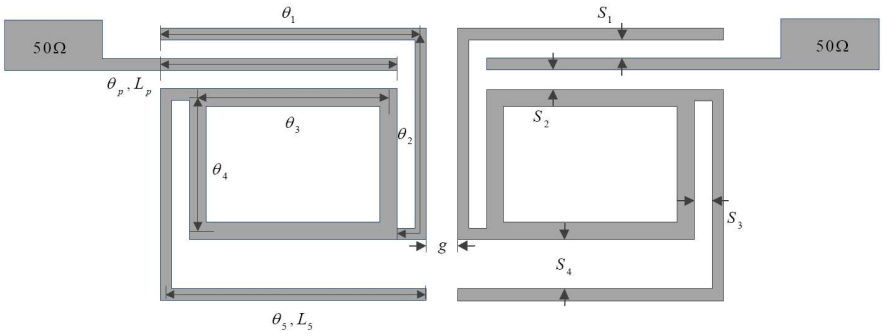

Figure 6. Layout of the proposed dual-band bandpass filter.

boundary of θ_2. We denote the electric lengths of the asymmetric perturbations as θ_1 and θ_5, which is depicted in Fig. 6. As analyzed in previous section, both of θ_1 and θ_5 can be used to control the resonances of the two passbands, while θ_1 is coupled to the feeder lines and θ_5 is independent. Consequently, θ_5 and S_4 are two extra freedoms for adjusting the resonances of two passbands. The fractional bandwidth (FBW) of each passband is determined by the external quality factor (Q_e) and coupling coefficients. The coupled section of θ_1 and the feeder line is denoted as θ_p, proper input/output external quality factor can be selected by adjusting θ_p and S_1. The coupling coefficients is controlled by the gap width of g. Thus the required bandwidth of each passband can be achieved by tuning θ_p, S_1 and g. Till now, the design procedure of the dual-band bandpass filter is as follows.

The first step is to obtain accurate physical dimensions of the

required resonant frequencies. It is done by tuning L_1, L_2, L_3, L_4, L_5 and S_4 slightly. At the same time, other dimensions should be arranged properly, i.e., the gap width of S_2 and S_3. The next step is to achieve the required bandwidth for the two passbands. A smaller coupling gap (g) results in a stronger coupling or smaller external quality factor. The gap width of S_1 and the coupling length of θ_p effect Q_e of both passbands. Various coupling strengths can be obtained by changing the physical dimensions. After the preceding two steps, dimensions of the dual-band bandpass filter are determined.

Figure 7 plots the simulated frequency responses of the proposed filter. From the figure, it can be found that there are two transmission zeros located at two sides of each passband. The reason is that the space between the input/output lines is 90° due to the cascaded structure, since the input line is coupled to one side of the loop resonator and the output line is coupled to the perturbation stub of the second resonator, while the perturbation stub of the second resonator is coupled to another side of the first loop resonator. Meanwhile, the two sides of the loop are vertical. Traditional ring resonator filters have two transmission zeros on both sides of the passband when the space between the input and output lines is 90° [13, 14].

According to the above discussion, the overall design procedure of this kind of filters can be summarized as follows,

1) Give the desired parameters (f_1, f_2, FBW_1 and FBW_2) of the dual-band filter.
2) Choose a proper normalized electric length ratio k, the initial value should be select in the experiential range of [1.2, 1.4].

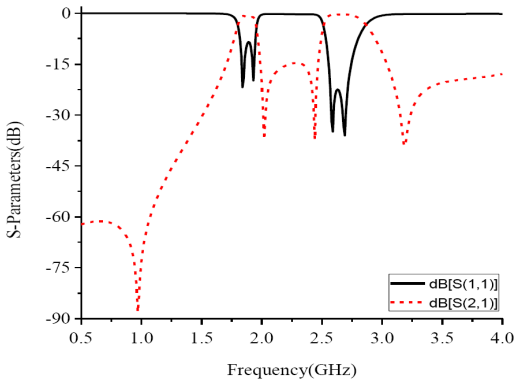

Figure 7. Simulated frequency response of the filter in Fig. 6. ($L_1 = 14.2\,\text{mm}$, $L_2 = 11.2\,\text{mm}$, $L_3 = 11.8\,\text{mm}$, $L_4 = 8.8\,\text{mm}$, $L_5 = 13.5\,\text{mm}$, $L_p = 13.6\,\text{mm}$, $S_1 = 0.2\,\text{mm}$, $S_2 = 0.6\,\text{mm}$, $S_3 = 0.4\,\text{mm}$, $S_4 = 2\,\text{mm}$, $g = 0.15\,\text{mm}$).

3) Find a suitable impedance ratio of R_Z from Fig. 3 so as to select line widths of the loop resonator and the perturbation stubs.
4) Plot the normalized resonant frequencies versus normalized stub length according to (3) and (4).
5) Read two normalized resonant frequencies from the plotted figure at the certain position of k.
6) Calculate the fundamental resonance f_0 of the loop resonator according to (5) and then obtain the wave-guided wavelength λ_0.
7) Define the initial dimensions of the filter, which should satisfy $L_3 + L_4 \approx \lambda_0/2$ and $(L_1 + L_2)/(L_3 + L_4) \approx k$.
8) Arrange other dimensions to ensure the resonances of the overall circuit.
9) Cascaded two resonators and adjust dimensions to obtain accurate resonances and fractional bandwidths.

Additionally, the second resonance of the filter can be easily adjusted by adding a patch perturbation in the corner of the loop, as shown in Fig. 8(a). The patch perturbation is equivalent to a capacitance of C_P, the perturbation C_P affects the even-mode resonance frequency (f_2) but has no relationship with the odd-mode one (f_1) [12, 15]. Fig. 8(b) demonstrates the resonances of the even-mode (f_2) and odd-mode (f_1) against perturbation size$p$. The odd-mode resonance (f_1) has a minor change because that the length of the transmission line adjacent to the perturbation patch is disturbed when the perturbation size changes [15].

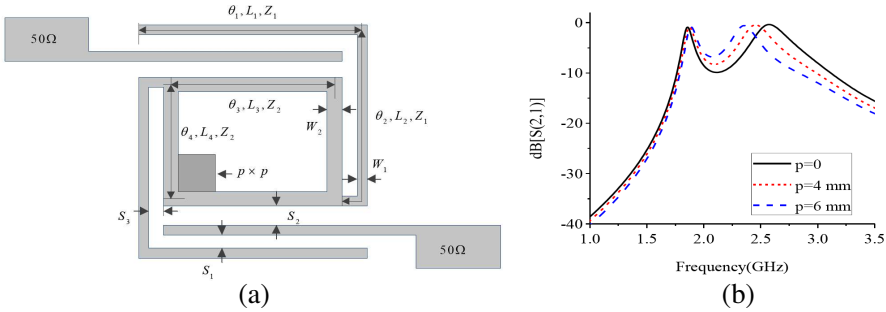

Figure 8. (a) Initial resonator with patch perturbation. (b) Simulated frequency responses of the even and odd mode against perturbation size p. (Dimensions are the same with those in Fig. 5).

3. RESULTS AND DISCUSSION

To verify the design principle, the filter centered at 1.9 and 2.6 GHz are fabricated on a substrate with dielectric constant $\varepsilon_r = 2.65$ and thickness $h = 1\,\text{mm}$. The attenuation out of the right side of the second passband is suppressed by a pair of additional spur-lines [16, 17], which can introduce transmission zeros at desired frequency. The filter configure with spur-lines is shown in Fig. 9(a). By optimizing the location of the spur-lines, final physical dimensions of the filter are determined as follows: $W_1 = 0.4\,\text{mm}$, $W_2 = 0.8\,\text{mm}$, $W_S = 0.4\,\text{mm}$, $L_1 = 14.2\,\text{mm}$, $L_2 = 11.2\,\text{mm}$, $L_3 = 11.8\,\text{mm}$, $L_4 = 8.8\,\text{mm}$, $L_5 = 13.5\,\text{mm}$, $L_p = 13.6\,\text{mm}$, $L_S = 12.5\,\text{mm}$, $S_1 = 0.2\,\text{mm}$, $S_2 = 0.6\,\text{mm}$, $S_3 = 0.4\,\text{mm}$, $S_4 = 2\,\text{mm}$, $d = 1\,\text{mm}$, $g = 0.15\,\text{mm}$. The total size of the filter is about $0.43\lambda_g \times 0.14\lambda_g$, where λ_g is the guided wavelength

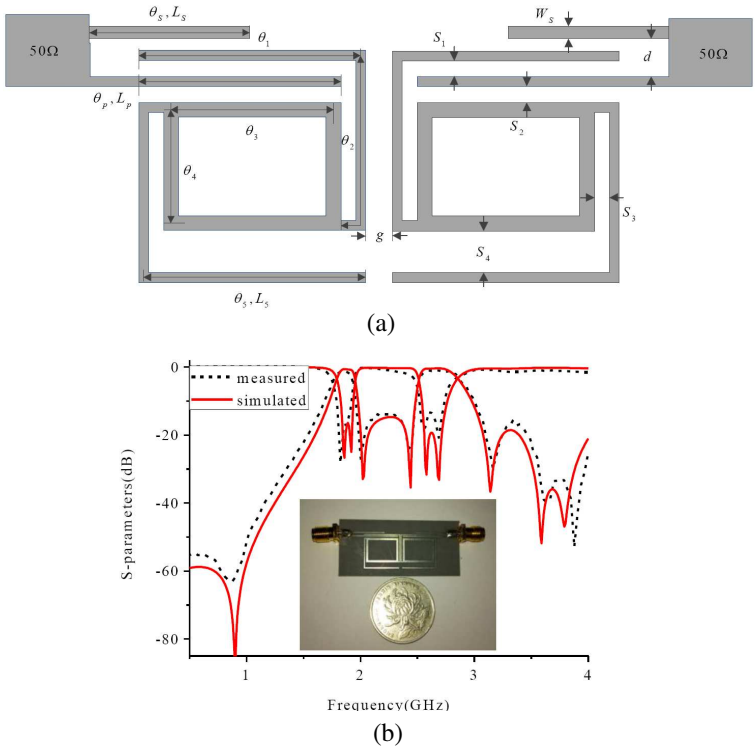

Figure 9. (a) Configuration of the proposed filter with spur-lines. (b) Comparison of the simulated and measured results of frequency responses, inserted figure is the fabricated photograph of the filter.

at the first resonant frequency (f_1). The simulation and measurement are accomplished by using IE3D. Fig. 9(b) depicts the simulated and measured results, which show good agreement. Fabricated photograph of the filter is inserted in Fig. 9(b). The first passband is centered at 1.86 GHz, with the 3 dB bandwidth of 9.2%, the insertion loss is measured to be 1.16 dB, the return loss is greater than −17 dB. Two transmission zeros are realized close to the passband edges at 0.87 and 2.0 GHz, which greatly improve the skirt selectivity.

The second passband is located at 2.59 GHz, the 3 dB bandwidth is 12.4%. The minimum insertion loss is measured to be 1.2 dB. The return loss within the passband is greater than 13 dB. Four transmission zeros are created at 2.44, 3.16, 3.65 and 3.88 GHz. They are near the passband edges and significantly enhance the rates of roll-off.

4. CONCLUSION

A second-order dual-mode dual-band bandpass filter has been proposed in this paper. Even and odd analysis method based on transmission theory is used to construct the resonant conditions of the filter. Detailed design procedure is provided to show how to design this kind of filters. To verify the working principle and the design method, a filter centered at 1.9 GHz and 2.6 GHz is fabricated. Simulated and measured results show good agreement.

ACKNOWLEDGMENT

This work was supported by the National High Technology Research and Development Program of China (863 Program) No. 2012AA01A308 and the National Natural Science Foundation of China (NSFC) under Project Nos. 61271017 and 61072017.

REFERENCES

1. Miyake, H., S. Kitazawa, T. Ishizaki, T. Yamada, and Y. Nagatom, "A miniaturized monolithic dual band filter using ceramic lamination technique for dual mode portable telephones," *IEEE MTT-S Int. Dig.*, Vol. 2, 789–792, Jun. 1997.
2. Wang, X.-H., B.-Z. Wang, and K. J. Chen, "Compact broadband dual-band bandpass filters using slotted ground structures," *Progress In Electromagnetics Research*, Vol. 82, 151–166, 2008.

3. Fan, J.-W., C.-H. Liang, and X.-W. Dai, "Design of cross-coupled dual-band filter with equal-length split-ring resonators," *Progress In Electromagnetics Research*, Vol. 75, 285–293, 2007.
4. Xue, W., C.-H. Liang, X.-W. Dai, and J.-W. Fan, "Design of miniature planar dual-band filter with 0° feed structures," *Progress In Electromagnetics Research*, Vol. 77, 493–499, 2007.
5. Ma, D.-C., Z.-Y. Xiao, L.-L. Xiang, X.-H. Wu, C.-Y. Huang, and X. Kou, "Compact dual-band bandpass filter using folded SIR with two stubs for WLAN," *Progress In Electromagnetics Research*, Vol. 117, 357–364, 2011.
6. Kuo, J.-T. and S.-W. Lai, "New dual-band bandpass filter with wide upper rejection band," *Progress In Electromagnetics Research*, Vol. 123, 371–384, 2012.
7. Kuo, J.-T., C.-Y. Fan, and S.-C. Tang, "Dual-wideband bandpass filters with extended stopband based on coupled-line and coupled three-line resonators," *Progress In Electromagnetics Research*, Vol. 124, 1–15, 2012.
8. Luo, S., L. Zhu, and S. Sun, "A dual-band ring-resonator bandpass filter based on two pairs of degenerate modes," *IEEE Trans. Microw. Theory Tech.*, Vol. 58, No. 12, 3427–3432, Dec. 2010.
9. Wu, G.-L., W. Mu, X.-W. Dai, and Y.-C. Jiao, "Design of novel dual-band bandpass filter with microstrip meander-loop resonator and CSRR DGS," *Progress In Electromagnetics Research*, Vol. 78, 17–24, 2008.
10. Chen, Z.-X., X.-W. Dai, and C.-H. Liang, "Novel dual-mode dual-band bandpass filter using double square-loop structures," *Progress In Electromagnetics Research*, Vol. 77, 409–416, 2007.
11. Zhao, L.-P., X.-W. Dai, Z.-X. Chen, and C.-H. Liang, "Novel design of dual-mode dual-band bandpass filter with triangular resonators," *Progress In Electromagnetics Research*, Vol. 77, 417–424, 2007.
12. Deng, K., B. Wu, S.-J. Sun, and C.-H. Liang, "Dual-band filter based on dual-stubs loaded square loop resonator," *Int. Conf. Microw. Millimeter Wave Technol., ICMMT — Proc.*, 1–3, May 2012.
13. Chiou, Y.-C., P.-S. Yang, J.-T. Kuo, and C.-Y. Wu, "Transmission zero design graph for dual-mode dual-band filter with periodic stepped-impedance ring resonator," *Progress In Electromagnetics Research*, Vol. 108, 23–36, 2010.
14. Matsuo, M., H. Yabuki, and M. Makimoto, "Dual-mode stepped-impedance ring resonator for bandpass filter applications," *IEEE*

Trans. Microw. Theory Tech., Vol. 49, No. 7, 1235–1240, Jul. 2007.

15. Fu, S., B. Wu, J. Chen, S.-J. Sun, and C.-H. Liang, "Novel second-order dual-mode dual-band filters using capacitance loaded square loop resonator," *IEEE Trans. Microw. Theory Tech.*, Vol. 60, No. 3, 477–483, Mar. 2012.
16. Wang, Y.-Z. and M.-L. Her, "Compact microstrip bandstop filters using stepped-impedance resonator (SIR) and spur-line sections," *IEE Proc., Microw. Antennas Propag.*, Vol. 153, 435–440, UK, Oct. 2006.
17. Zhang, X.-Y., J.-X. Chen, Q. Xue, and S.-M. Li, "Dual-band bandpass filters using stub-loaded resonators," *IEEE Microw. Wireless Compon. Lett.*, Vol. 17, No. 8, 583–585, Aug. 2007.